JOURNAL OF MATERIALS SCIENCE 33 (1998) 895–900

Relaxation characteristics of strontium barium niobate ferroelectric ceramics

HUIQING FAN*, LIANGYING ZHANG, XI YAO
Electronic Materials Research Laboratory, Xi'an Jiaotong University, Xi'an 710049, People's Republic of China

The complex dielectric response of tungsten bronze $Sr_{1-x}Ba_xNb_2O_6$ (SBN $(1-x)/x$, $x = 0.40$, 0.50, and 0.60) relaxor ferroelectric ceramics has been carefully studied as a function of temperature between -180 and 450 °C. Three distinct relaxation features were observed in all the compositions. The thermal hysteresis of dielectric maximum was considered to be associated with "lock in" of the incommensurate phase. It was confirmed by investigation of the Curie–Weiss behaviour in the higher temperature range. In addition, it was found that the weakness of the dielectric dispersion below the ferroelectric–paraelectric phase transition temperature can be induced by ageing and poling. These results are discussed in terms of the polarization fluctuation and metastability of polar microregions. © *1998 Chapman & Hall*

1. Introduction

The vast group of compounds called relaxor ferroelectrics has been extensively studied for more than 30 y, particularly due to their technological importance [1–3]. In contrast to normal ferroelectrics, relaxor ferroelectrics possess a strong frequency-dependent dielectric response characteristic of a relaxation process, and the temperature of the dielectric permittivity maximum was found to shift to higher temperature with increasing measurement frequency. There is a need for understanding the reasons for their electrical properties, especially their dielectric relaxation characteristics.

Perovskite lead magnesium niobate (PMN) for many years has been a classical subject of relaxor ferroelectrics study [4–6]. Recently, another distinct family of relaxor ferroelectrics, having the tungsten bronze structure, has been subject to an increasing trend of research and development [7–10]. Strontium barium niobate solid solutions ($Sr_{1-x}Ba_xNb_2O_6$, $0.25 < x < 0.75$), exhibiting a structure closely related to the tetragonal tungsten bronze structure (P_4bm or $4mm$), are of immense importance in many technological applications such as pyroelectric detectors and electrooptic and surface acoustic wave (SAW) devices [7, 11–14]. In fact, the dielectric relaxation of single crystals of SBN relaxor ferroelectrics as a function of composition and crystallographic orientation have been studied thoroughly over a wide temperature range (-263–400 °C) in the literature [7, 15–18]. Most interesting studies have also related the low-temperature dielectric anomaly with incommensurate structures which were observed in many tungsten bronze ferroelectrics [19–21]. A complex sequence of transformations involving incommensurate structures seems to be a common feature of many tungsten bronze ferroelectrics [18, 22].

The purpose of this study was to investigate the dielectric relaxation characteristics of SBN relaxor ferroelectric ceramics as a function of temperature on which relatively scant information is available [23–26]. The ageing and poling behaviour of dielectric response of SBN relaxor ferroelectric ceramics have also been studied for comparison. In addition, polar nano microregion (PMR) was used to discuss the results briefly.

2. Experimental procedure

2.1. Sample preparation

A conventional mixed-oxide technique was used to prepare the $Sr_{1-x}Ba_xNb_2O_6$ samples. The batches were prepared using reagent-grade $SrCO_3$, $BaCO_3$, and Nb_2O_5. The chemicals were weighed and ball milled for 24 h with ZrO_2 media and alcohol. Pellets of mixed powder pressed using low pressure were calcined for 2 h at 1380 °C. The calcined pellets were then cracked and mixed with ZrO_2 media and alcohol by planetary milling. The dried mixtures were then pelletized under 10 MPa pressure and sintered in a crucible at 1460 °C for 1 h. The sintered samples were all characterized with tetragonal tungsten bronze phase by X-ray powder diffraction (XRD).

The $Sr_{1-x}Ba_xNb_2O_6$ composition samples chosen for study included $x = 0.40$, 0.50, and 0.60, (designated as SBN60/40, 50/50, and 40/60, respectively). Samples for electrical measurements were electroded with low-temperature-fired silver paint.

* Author to whom all correspondence should be addressed.

2.2. Dielectric and pyroelectric properties measurement

The weak-field dielectric response was measured by using a Hewlett Packard 4274A LCR meter which can cover a frequency range from 100 Hz to 100 kHz. For low-temperature measurements, samples were placed in a test chamber, which can be operated between −196 and 250 °C. The four-terminal pair configuration, which was connected together directly to the electrodes of the sample, was used to increase the measuring accuracy. Before the measurement, a standard calibration was performed to remove any stray capacitance, lead and contact resistance. The temperature was measured using a Hewlett Packard 3455A digital voltage meter via a platinum resistance thermometer mounted directly on the ground electrode of the sample fixture. The amplitude level of the signal was 5 V cm^{-1} The temperature controllers, HP3455A, HP4274A were controlled with a PC computer.

The dielectric response was measured as a function of temperature between −100 and 200 °C. Before each cooling run, the sample was first heated up to 200 °C to allow free reorientation of polarization induced by polishing and ageing. Cooling and heating runs were performed at the rate of 1 °C min^{-1}. The high-temperature dielectric data were obtained by putting the samples in a small furnace specifically equipped for such measurement. The temperature range was between 500 °C and room temperature. Data were taken by cooling the samples from high temperature to room temperature at a rate of 1 °C min^{-1}.

Samples were aged under open-circuit conditions at 5–18 °C room temperature for 1 y, then the temperature was lowered to −180 °C, and the sample was measured during heating at a rate of 1 °C min^{-1}. When poling is required, the sample was poled applying a d.c. electric field of 20 kV cm^{-1} at 200 °C for 15 min and cooled to −180 °C under the electric field. After removing the field, and shorting the electrodes for 10 min to release the surface charge, measurements were made by measuring the discharge current on heating using a HP4140B PA meter and the dielectric response separately [27].

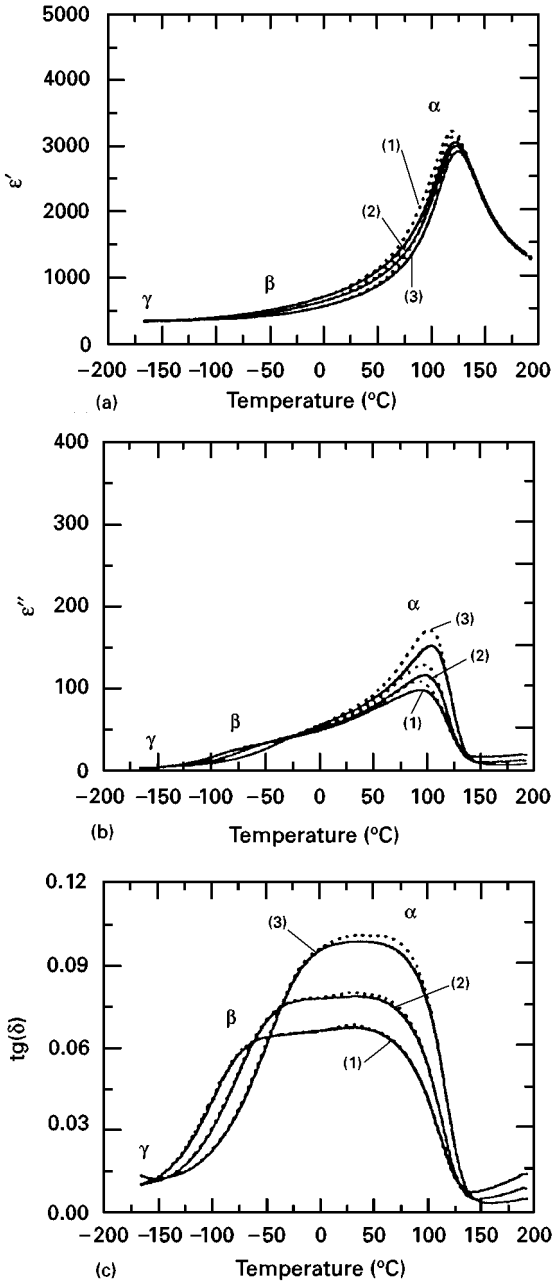

Figure 1 Frequency dependence of dielectric response as a function of temperature for SBN40/60 upon (· · · ·) cooling and (—) heating measurements: (a) real component, (b) imaginary component, (c) phase component. (1) 1 kHz, (2) 10 kHz, (3) 100 kHz.

3. Results and discussion

3.1. Dielectric relaxation properties

The complex dielectric permittivity, $\varepsilon = \varepsilon' - i\varepsilon''$, and the loss factor, $\mathrm{tg}\delta = \varepsilon''/\varepsilon'$, as a function of temperature at various measurement frequencies, are shown in Figs 1a–c to 3a–c for SBN40/60, 50/50, and 60/40, respectively, upon heating and cooling measurements. Three distinct relaxation features were observed in all the compositions. These dispersive phenomena were named α, β, and γ, respectively. The α dielectric dispersion appeared near the Curie range; it is a diffuse nature of the ferroelectric phase transition. An interesting relaxation feature, β, can be clearly seen in temperature range of ε″ and tgδ, which showed a strong Debye-like dielectric dispersion. Another Debye-like relaxation anomaly, γ, was found at a temperature lower than about −150 °C for all the compositions. Fig. 4 shows the pyroelectric current and polarization calculated by back integration for SBN50/50 between −165 and 150 °C. Two small and a sharp pyroelectric current peaks were clearly observed, which all coincided with the three dielectric dispersive phenomena.

The α dielectric anomaly is due to the temperature and frequency dependencies of dielectric permittivity of relaxor ferroelectrics near the ferroelectric–paraelectric phase transition which have been studied exclusively as characteristics of relaxor ferroelectrics. With increasing strontium content, the peak value of the real component ε′ can be seen to be increased with enhanced dielectric dispersion, and the temperature of the maximum decreased. Similar compositional dependencies of the corresponding

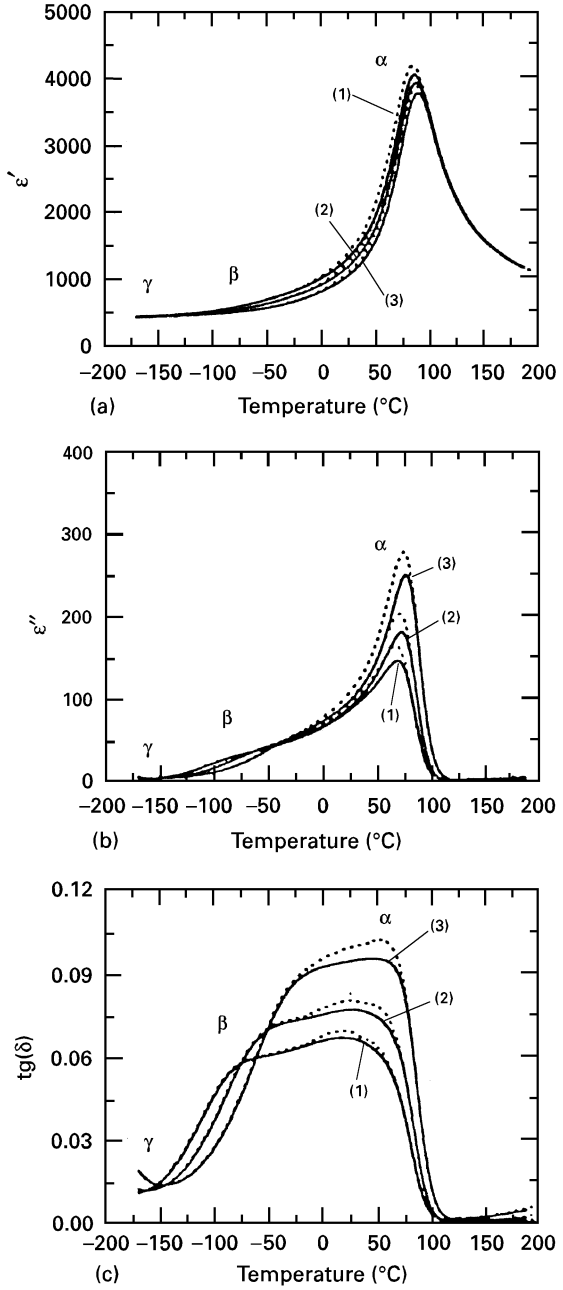

Figure 2 Frequency dependence of dielectric response as a function of temperature for SBN50/50 upon (· · · ·) cooling and (—) heating measurements: (a) real component, (b) imaginary component, (c) phase component. (1) 1 kHz, (2) 10 kHz, (3) 100 kHz.

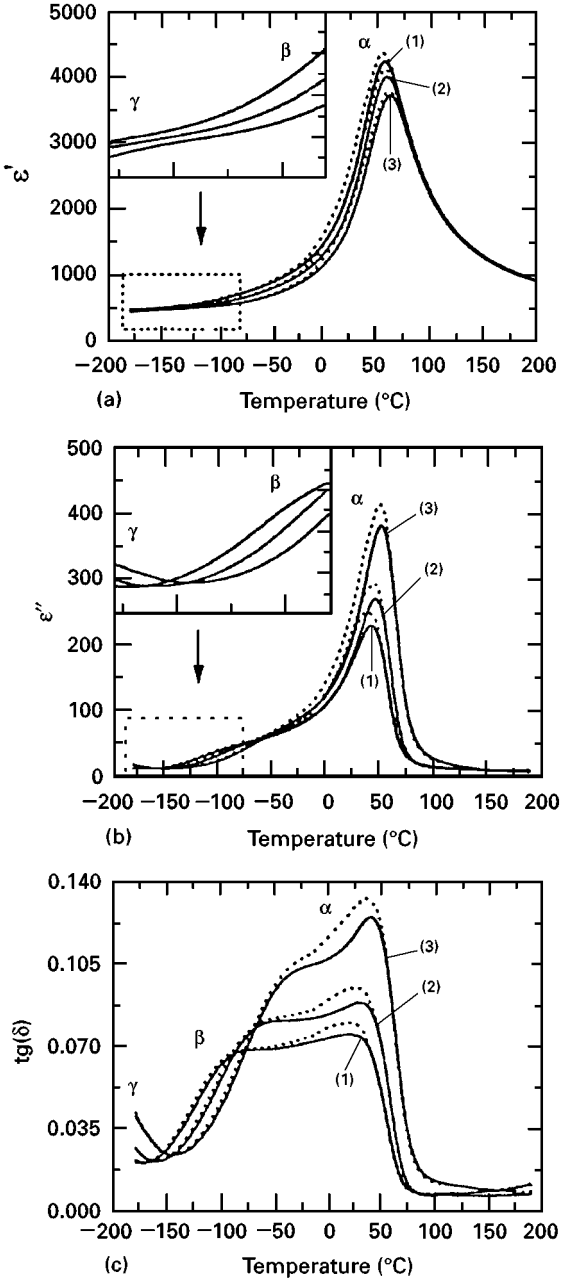

Figure 3 Frequency dependence of dielectric response as a function of temperature for SBN60/40: (a) real component, (b) imaginary component, (c) phase component. (1) 1 kHz, (2) 10 kHz, (3) 100 kHz. (—) Heating, (· · · ·) cooling.

imaginary component ε'' can also be seen. The stronger relaxor characteristics with increasing strontium content, undoubtedly reflect enhanced disorder [28]. It should be noted that the most interesting relaxation character was found in the α range for all the compositions. Hysteresis effects are clearly evident below the maximum in the dielectric response, the magnitude of this hysteresis cannot be absent at a lower rate of measurement. The hysteresis effects in this field may be attributed to the "lock in" of incommensurate phase (incommensuration) with the ferroelectric–paraelectric transition [29]. This will be confirmed by the β dielectric anomaly and investigation of the Curie–Weiss behaviour in the higher temperature range.

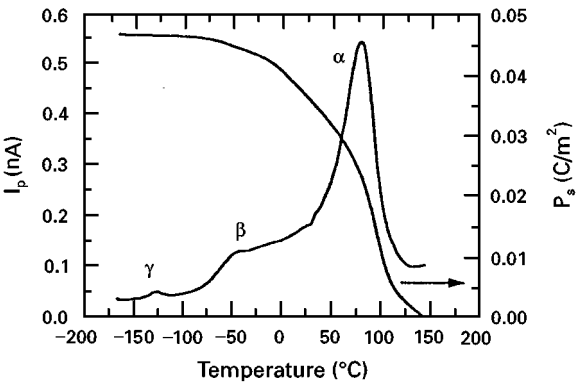

Figure 4 The pyroelectric current and polarization calculated by back integration for SBN50/50.

The β dielectric dispersion behaviour is believed to be further experimental evidence corresponding to the earlier report of the incommensurate superlattice structure found in the SBN system. Evidence for an incommensurate–commensurate phase transition at around $-75\,^{\circ}C$ in SBN50/50 single crystal was reported by Bursill and Lin [19], indicated by incommensurate superlattice spacing along $k_{1\,1\,0}$, detected by high-resolution transmission electron microscopy (HRTEM). The crystallographic basis of this incommensurate superlattice comes from the modulation of the O-ions in the $(0, 0\ z/2)$ plane that causes cell doubling in the c-direction and, in turn, gives rise to the tilting of the oxygen octahedral in the a–b plane and, therefore, the orthorhombic superlattice. With increasing Sr/Ba ratio, the modulation would become very weak and thus the temperature range of the β dielectric dispersion anomaly will decrease. It is suggested that both α and β phenomena are related to the A-site cation ordering in this solid-solution system.

The γ dielectric dispersion phenomenon is presumably related to the polarization fluctuation "freezing-in" originating from the relaxor nature of SBN solid solution. Based on the thermally agitated local polarization fluctuation model proposed by Guo *et al.* [30], this low-temperature relaxation behaviour is explained. In SBN ferroelectric ceramics, the fluctuation component of the polarization can take place not only in the high-temperature paraelectric phase, but also in the low-temperature ferroelectric phase. It underlines, in general, that tungsten bronze structure is more flexible to allow the coupling between the nano-scale polar microregions in the ferroelectric matrix. This idea can be confirmed by investigations of the poling and ageing behaviour of SBN ferroelectric ceramics.

3.2. Curie–Weiss investigations

Fig. 5 shows the Curie–Weiss law-fitting curve at 1 kHz for SBN60/40, 50/50 and 40/60. No deviations from Curie–Weiss behaviour above the dielectric permittivity maximum can be seen for all the compositions. The extrapolated Curie temperature nearly coincides with the temperature of the dielectric

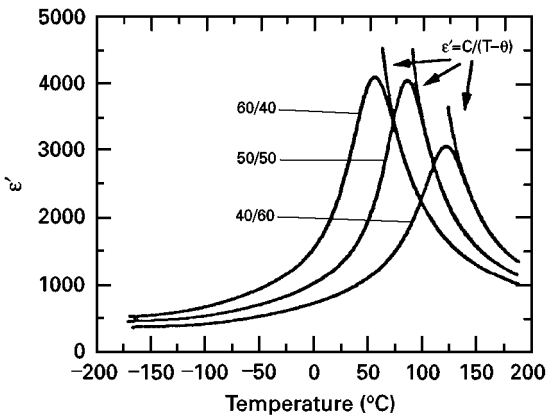

Figure 5 The 1 kHz dielectric permittivity as a function of temperature for SBN60/40, 50/50 and 40/60, where the points are the data and the solid line is the fitting to the Curie–Weiss law.

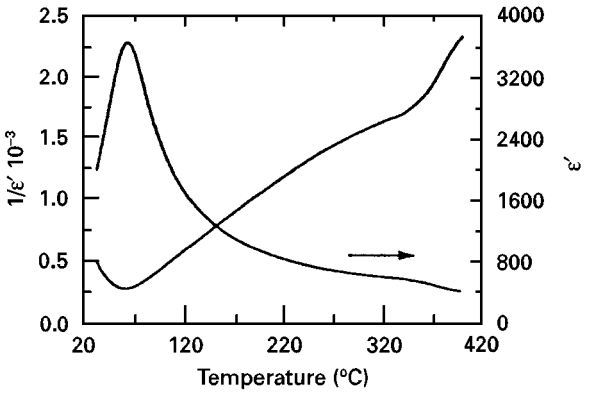

Figure 6 The 100 kHz dielectric permittivity and inverse permittivity for SBN60/40 from 400 °C to room temperature.

permittivity maximum for each composition. The calculated values of the Curie constant were all of the order of 10^5. This type of behaviour is in distinct disagreement with that of lead-based perovskite relaxor ferro-electrics where strong deviations from Curie–Weiss behaviour are observed until a temperature far above the dielectric maximum.

To investigate more thoroughly the Curie–Weiss behaviour of SBN relaxor ferroelectric ceramics, measurements were made over a higher temperature interval. Plots of dielectric permittivity and inverse permittivity of SBN60/40 from 400 °C to room temperature are shown in Fig. 6. It can be clearly seen that the inverse permittivity behaviour becomes linear until $\sim 350\,^{\circ}C$ with cooling measurement. Incommensuration in SBN 60/40 is known to exist until a temperature far above the Curie range. It is possible that the change in the slope in the Curie–Weiss behaviour is a reflection of the normal–incommensurate transformation. This transformation temperature coincides with the temperature of existence of local polarization in SBN found by Bhalla *et al.* [16] from the quadratic temperature dependence of the thermal expansion. In lead-based perovskite relaxor ferroelectrics, the strong deviation from Curie–Weiss behaviour reflects the development of correlation between stable nano-scale polar microdomains [6]. At high temperatures, the disordering effect of temperature prevents strong couplings; however, as the temperature decreases, a correlation develops as the volume fraction of polar regions increases and the thermal disordering effects decrease. In SBN relaxor ferroelectrics, discommensurates possibly act to destroy the long-range dipolar interactions between a polar microregion in the paraelectric phase.

3.3. Dielectric ageing and poling behaviour

Fig. 7 shows the dielectric response of aged and fresh SBN60/40 relaxor ferroelectric ceramics. The dielectric permittivity and loss for aged samples are all less than for the fresh sample, especially near the room-temperature range, and the dispersion of dielectric permittivity was reduced from room temperature to the Curie temperature. Fig. 8 gives the dielectric response of poled and unpoled SBN50/50 relaxor

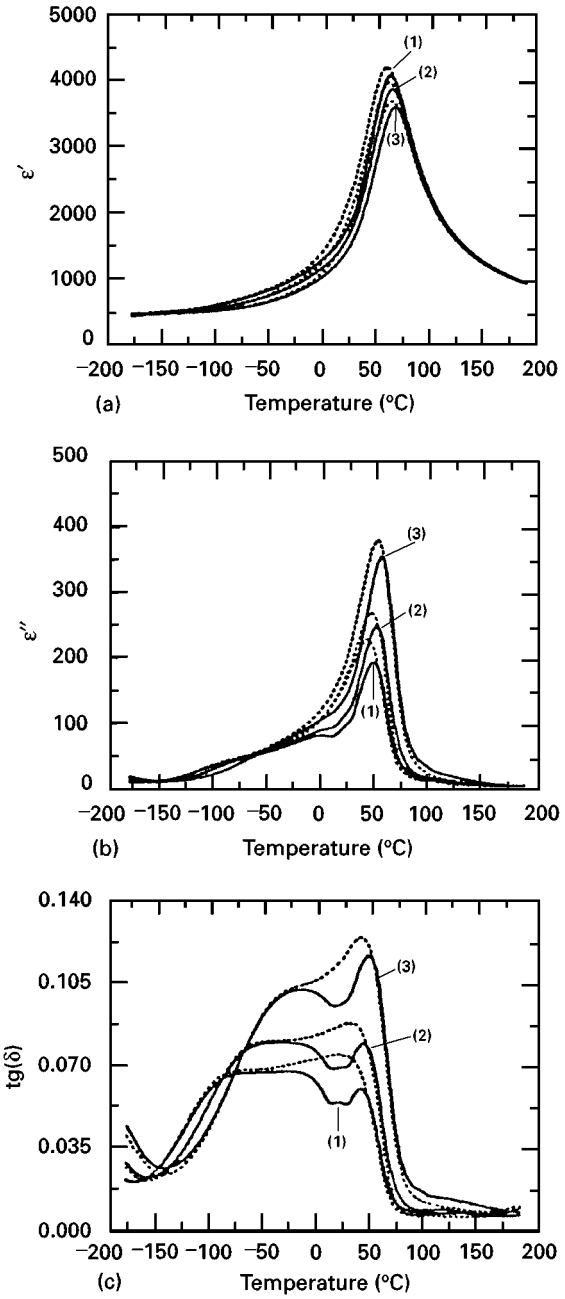

Figure 7 Frequency dependence of dielectric response as a function of temperature for aged SBN60/40: (a) real component, (b) imaginary component, (c) phase component. (· · · ·) Fresh, (—) aged. (1) 1 kHz, (2) 10 kHz, (3) 100 kHz.

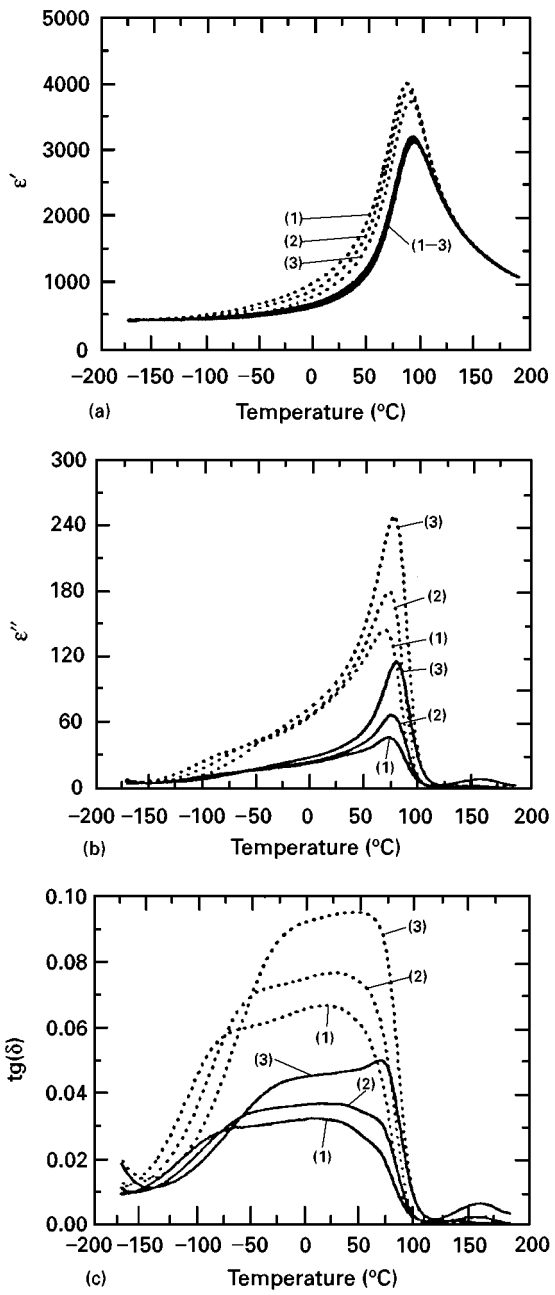

Figure 8 Frequency dependence of dielectric response as a function of temperature for poled SBN50/50: (a) real component, (b) imaginary component, (c) phase component. (· · · ·) unpoled, (—) poled . (1) 1 kHz, (2) 10 kHz, (3) 100 kHz.

ferroelectric ceramics. The dielectric permittivity and loss for the poled sample are all less than for the unpoled sample, and the dispersion of dielectric permittivity almost disappeared in the whole ferroelectric temperature range. When SBN ceramics are aged and allowed to stand for a long time, the nano-scale polar microregions in the ferroelectric matrix can transform into ferroelectric macrodomains to stabilize themselves to a low-energy state. During the poling process, a field-induced relaxor-normal ferroelectric transitions occurred. That is, the nano-scale polar microregions in the ferroelectric matrix can transform into ferroelectric macrodomains during the poling process. As discommensurates exist in SBN ferroelectric ceramics, the field-induced ferroelectric macrodomains depoled up to the Curie temperature, which is a very different behaviour from that of the perovskite relaxor ferroelectrics.

4. Conclusions

1. Three distinct relaxation features were observed in the complex dielectric response of tungsten bronze $Sr_{1-x}Ba_xNb_2O_6$ (SBN$(1-x)/x$, $x = 0.40$, 0.50, and 0.60) relaxor ferroeletric ceramics.

2. It is suggested that the incommensurate phase plays an important role in dielectric relaxation of $Sr_{1-x}Ba_xNb_2O_6$ relaxor ferroeletric ceramics.

3. Metastability of polar microregions in relaxor ferroelectrics was confirmed by the ageing and poling behaviour of $Sr_{1-x}Ba_xNb_2O_6$ relaxor ferroelectric ceramics.

Acknowledgement

This research was fully supported by the National Natural Science Foundation of China (no. 59232042).

References

1. G. A. SMOLENSKII, *J. Phys. Soc. Jpn* **28** (Suppl) (1970) 26.
2. L. E. CROSS, *Ferroelectrics* **76** (1987) 241.
3. G. SCHMIDT, *Phase Transitions* **20** (1990) 127.
4. G. BURNS and F. H. DACOL, *Solid State Commun.* **48** (1983) 853.
5. A. D. HILTON, C. A. RANDALL, D. J. BARBER and T. R. SHROUT, *Ferroelectrics* **93** (1989) 379.
6. D. VIEHLAND, S. J. JANG, M. WUTTING and L. E. CROSS, *J. Appl. Phys.* **68** (1990) 2916.
7. A. M. GLASS, *ibid.* **40** (1969) 4699.
8. T. IDEKA and I. FUJIMURA, *Jpn J. Appl. Phys.* **13** (1974) 57.
9. Y. XU, Z. LI, W. LI, H. WANG and H. CHEN, *Phys. Rev. B* **40** (1989) 11902.
10. C. A. RANDALL, R. GUO, A. S. BHALLA and L. E. CROSS, *J. Mater. Res.* **6** (1991) 1720.
11. P. V. LENZO, E. G. SPENCER and A. A. BALLMAN, *Appl. Phys. Lett.* **11** (1967) 191.
12. S. SINGH, D. A. DRAEGERT and J. E. GEUSIC, *Phys. Rev. B* **2** (1970) 2709.
13. R. R. NEURGAONKAR, W. F. HALL, J. R. OLIVER, W. W. HO and W. K. CORY, *Ferroelectrics* **87** (1988) 167.
14. A. S. BHALLA, R. GUO, G. BURNS, F. DACOL and R. R. NEURGAONKAR, *Phys. Rev. B* **36** (1987) 2030.
15. J. R. OLIVER, R. R. NEURGAONKAR and L. E. CROSS, *J. Appl. Phys.* **64** (1988) 37.
16. A. S. BHALLA, R. GUO, L. E. CROSS, G. BURNS, F. DACOL and R. R. NEURGAONKAR, *J. Appl. Phys.* **71** (1992) 5591.
17. J. M. POVOA, R. GUO and A. S. BHALLA, *Ferroelectrics* **158** (1994) 283.
18. D. VIEHLAND, Z. XU and W. H. HUANG, *Philos. Mag. A* **71** (1995) 205.
19. L. A. BURSILL and P. J. LIN, *Philos. Mag. B* **54** (1986) 157.
20. *Idem*, *Acta Crystallogr. B* **43** (1987) 49.
21. C. MANOLIKAS, *Phys. Status Solidi*(*a*) **68** (1981) 49.
22. C. MANOLIKAS, J. SCHNECK, J. TOLEDANO, J. KIAT and G. CALVARIN, *Phys. Rev. B* **35** (1987) 8884.
23. K. NAGATA, Y. YAMAMOTO, H. IGARASHI and K. OKAZAKI, *Ferroelectrics* **38** (1981) 853.
24. T. KIMURA, S. MIYAMOTO and T. YAMAGUCHI, *J. Amer. Ceram. Soc.* **73** (1990) 127.
25. B. JIMENEZ, C. ALEMANY, J. MENDIOLA and E. MAURER, *J. Phys. Chem. Solids* **46** (1985) 1383.
26. S. B. DESHPANDE, H. S. POTDAR, P. D. GODBOLE and S. K. DATE, *J. Amer. Ceram. Soc.* **75** (1992) 2581.
27. R. L. BYER and C. B. ROUNDY, *Ferroelectrics* **3** (1972) 333.
28. M. E. LINES and A. M. GLASS, "Principles and Application of Ferroelectrics and Related Materials" (Clarendon Press, Oxford, 1977) p. 291.
29. R. BLINC and A. P. LEVANYUK, "Incommensurate Phases in Dielectrics", Vol. 1 (North-Holland, Amsterdam, 1986).
30. R. GUO, A. S. BHALLA, C. A. RANDALL and L. E. CROSS, *J. Appl. Phys.* **67** (1990) 6405.

Received 21 April
and accepted 24 September 1997